Definitive Band Gaps for Single-Wall Carbon Nanotubes

Yuki Matsuda, Jamil Tahir-Kheli, and William A. Goddard III.*

Materials and Process Simulation Center, California Institute of Technology, California 91125

*Author to whom correspondence should be addressed. Phone: (626) 395-2731; Fax: (626) 585-0918. E-mail: wag@wag.caltech.edu

Supporting Information

Table S1. Structural Parameters after the Force Field Optimization and the Band Gaps of Zigazag, Armchair, and Chiral SWNTs Calculated Using the B3LYP Functional

n[a]	m[a]	atoms / unit cell	diameter (nm)	periodicity[b] (nm)	B3LYP E_g (eV)	experimental E_g (eV)
5	0	20	0.404	0.423	0.00	
6	0	24	0.489	0.425	0.00	
7	0	28	0.577	0.426	0.927	
8	0	32	0.641	0.426	1.283	
9	0	36	0.713	0.427	0.079	0.080 ± 0.005[c]
10	0	40	0.796	0.427	1.081	
11	0	44	0.869	0.427	1.139	
12	0	48	0.951	0.427	0.041	0.042 ± 0.004[c]
13	0	52	1.026	0.427	0.865	
14	0	56	1.107	0.428	0.890	
15	0	60	1.182	0.428	0.036	0.029 ± 0.004[c]
16	0	64	1.253	0.428	0.785	
17	0	68	1.339	0.428	0.734	
18	0	72	1.420	0.428	0.028	
19	0	76	1.496	0.428	0.617	
20	0	80	1.577	0.428	0.618	
21	0	84	1.655	0.428	0.021	
24	0	96	1.855	0.428	0.00	
25	0	100	1.967	0.428	0.477	
26	0	104	2.048	0.428	0.473	
27	0	108	2.217	0.428	0.00	
30	0	120	2.317	0.428	0.00	

31	0	124	2.439	0.428	0.388	
32	0	128	2.519	0.428	0.384	
5	5	20	0.557	0.247	0.00	
6	6	24	0.686	0.247	0.00	
10	10	40	1.366	0.247	0.00	0.00 [c]
8	2	57	0.725	6.523	0.00	
11	5	268	1.121	2.022	0.00	
15	5	260	1.422	1.542	0.66	0.50 – 0.60 ± 0.1 [d]
14	7	196	1.460	1.132	0.65	0.50 – 0.60 ± 0.1 [d]
16	4	112	1.446	0.653	0.00	
15	6	156	1.478	0.891	0.00	

[a] Chiral vectors, $C_h = (n, m)$.
[b] Periodicity of unit cell in SWNT along direction.
[c] Ref. 1.
[d] Ref. 18.

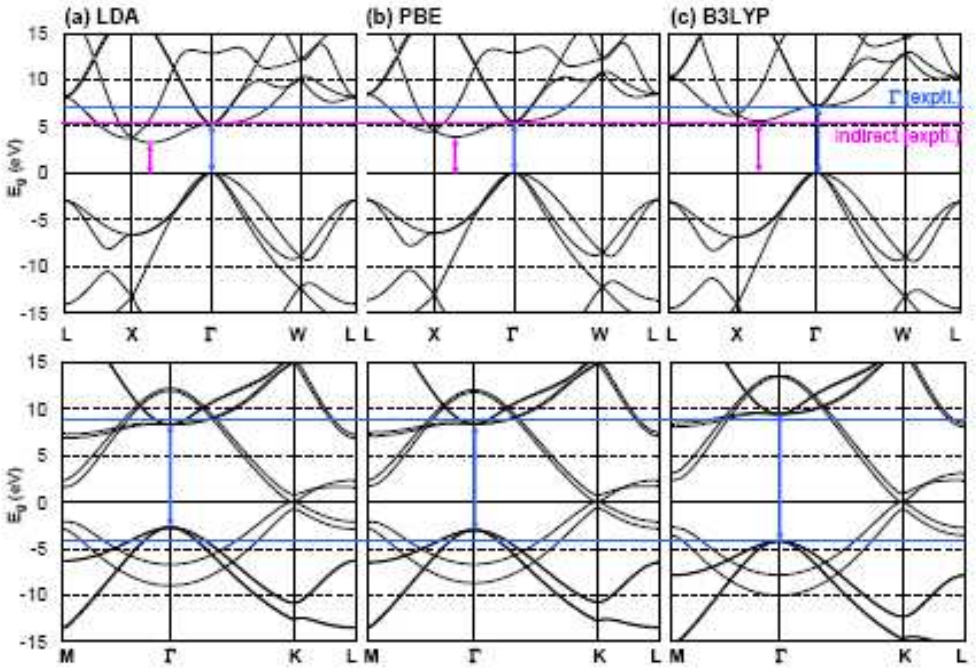

Figure S1. Band structures of diamond (top) and graphite (bottom) calculated by (a) LDA, (b) PBE, and (c) B3LYP. Experimental direct band gaps at Γ point (blue) and indirect band gaps (pink) are shown. The calculated and experimental band gaps are given in Table 1.

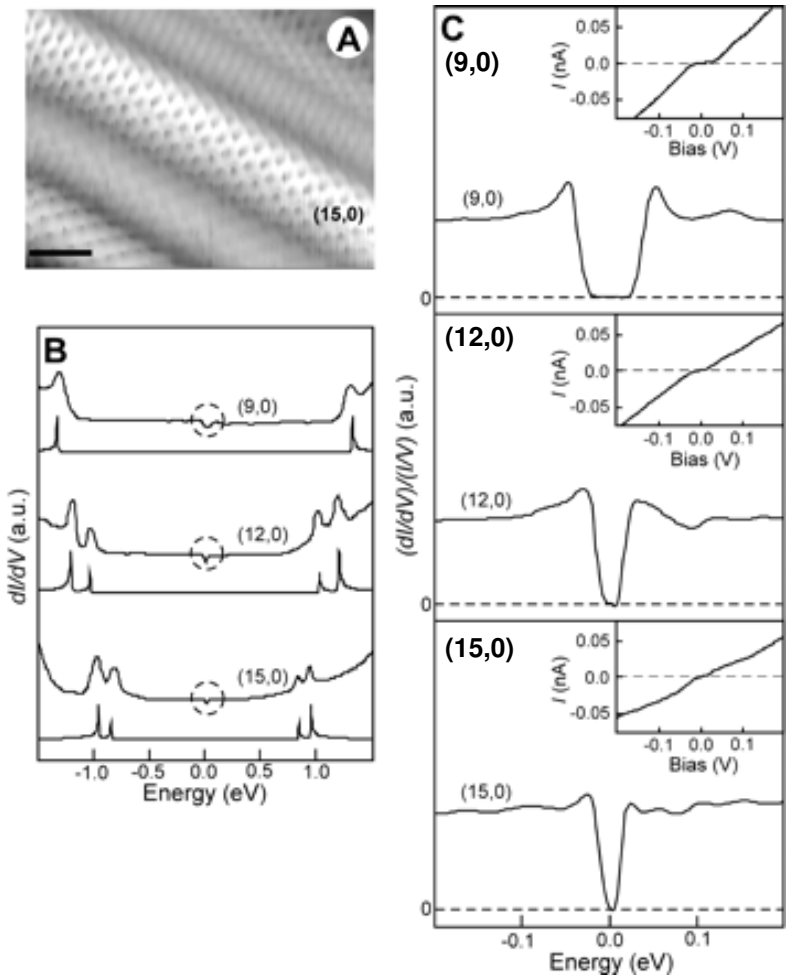

Figure S2. The STM measurements referred to in this paper were carried out in ultrahigh vacuum at ~5 K on SWNT samples supported on Au(111) substrates. To ease comparison with our calculated results, we extracted the figures and figure captions from the original paper by Lieber et al.[1] Atomic structure and spectroscopy of "metallic" zigzag SWNTs. (A) Typical atomically resolved STM image of a (15,0) SWNT. The image was recorded in the constant-current mode with bias voltage of 0.65 V and current *I* of 0.15 nA. (Scale bar: 1 nm). (B) Tunneling conductance data, *dI*/*dV*, for different zigzag SWNTs, with corresponding calculated DOS shown below each experimental curve in

arbitrary units (a.u.). The data were recorded as the in-phase component of *I* directly by a lock-in amplifier with a 7.37-kHz modulation signal of 2 mV peak-to-peak amplitude to the bias voltage. The new features in the low-energy region of the (9,0), (12,0), and (15,0) tubes are highlighted by dashed circles. (C) Typical high-resolution normalized conductance (*dI/dV*)/(*I/V*) curves and measured *I–V* curves (insets) for (9,0), (12,0), and (15,0) tubes, respectively. The (*dI/dV*)/(*I/V*) curves were calculated from *dI*/*dV* and *I–V* data.

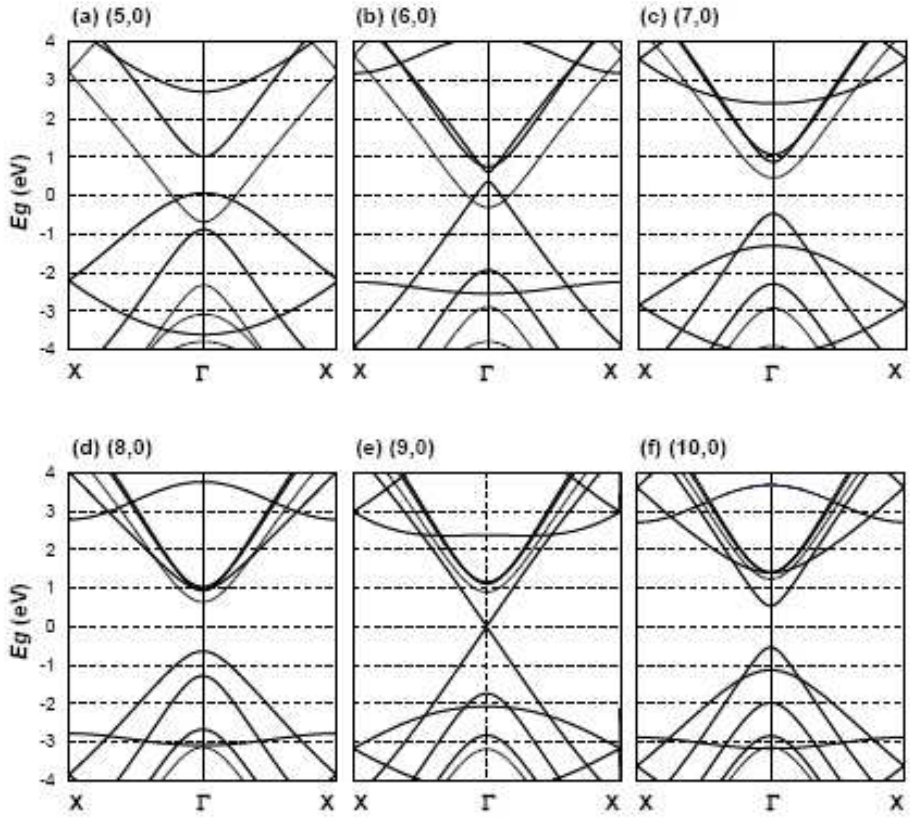

Figure S3-1. Band structures of zigzag SWNTs calculated using the B3LYP functional. (a) (5,0), (b) (6,0), (c) (7,0), (d) (8,0), (e) (9,0), and (f) (10,0). According to the chiral vector rules, (5,0) would be a semiconductor, however we find that strong distortions resulting from a small diameter makes it metallic. We find that (9,0) is metallic but there is a small band gap at the Fermi energy as shown in Figure 2.

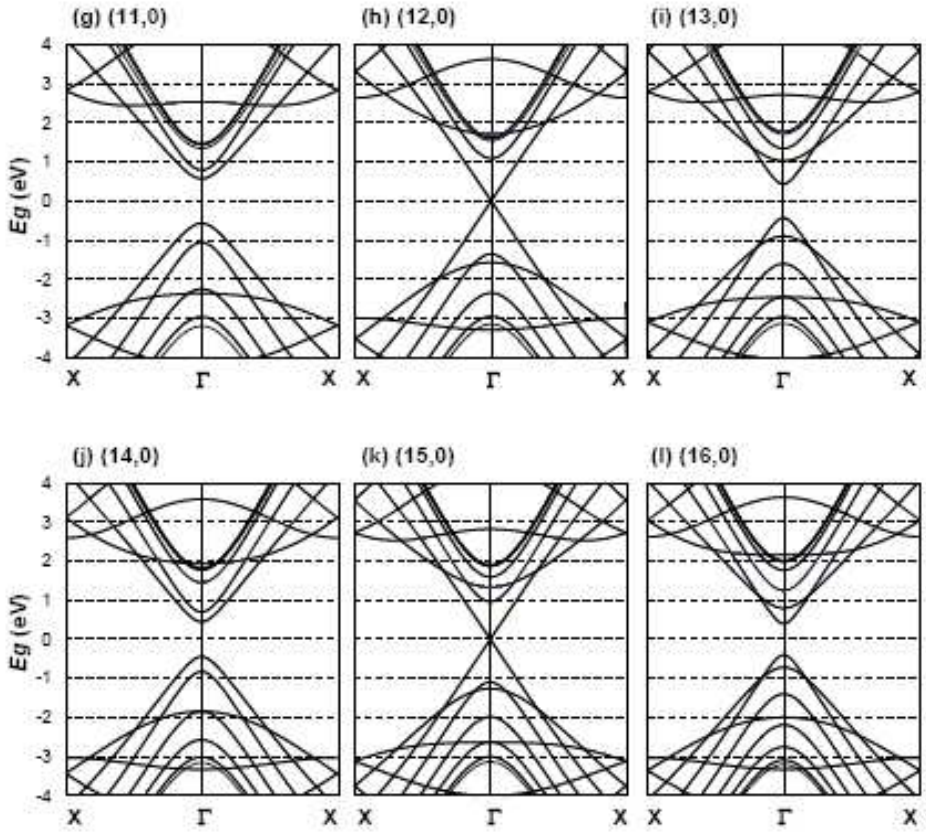

Figure S3-2. Band structures of zigzag SWNTs calculated using the B3LYP functional. (g) (11,0), (h) (12,0), (i) (13,0), (j) (14,0), (k) (15,0), and (l) (16,0). According to the chiral vector rules, (12,0) and (15,0) are metallic but we find small band gaps at the Fermi energy as shown in Figure 2.

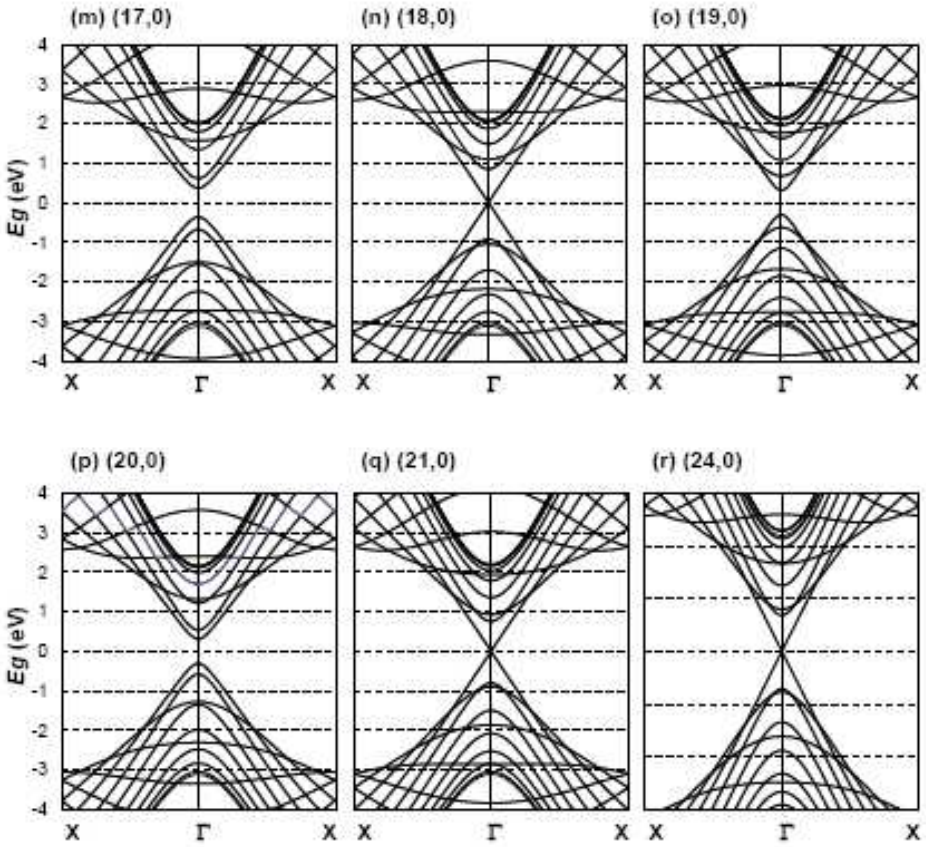

Figure S3-3. Band structures of zigzag SWNTs calculated using the B3LYP functional. (m) (17,0), (n) (18,0), (o) (19,0), (p) (20,0), (q) (21,0), and (r) (24,0).

According to the chiral vector rules, (18,0) and (21,0) are metallic but we find small band gaps at the Fermi energy as shown in Table 2. However, (24,0) shows metallic properties again (Figure 2).

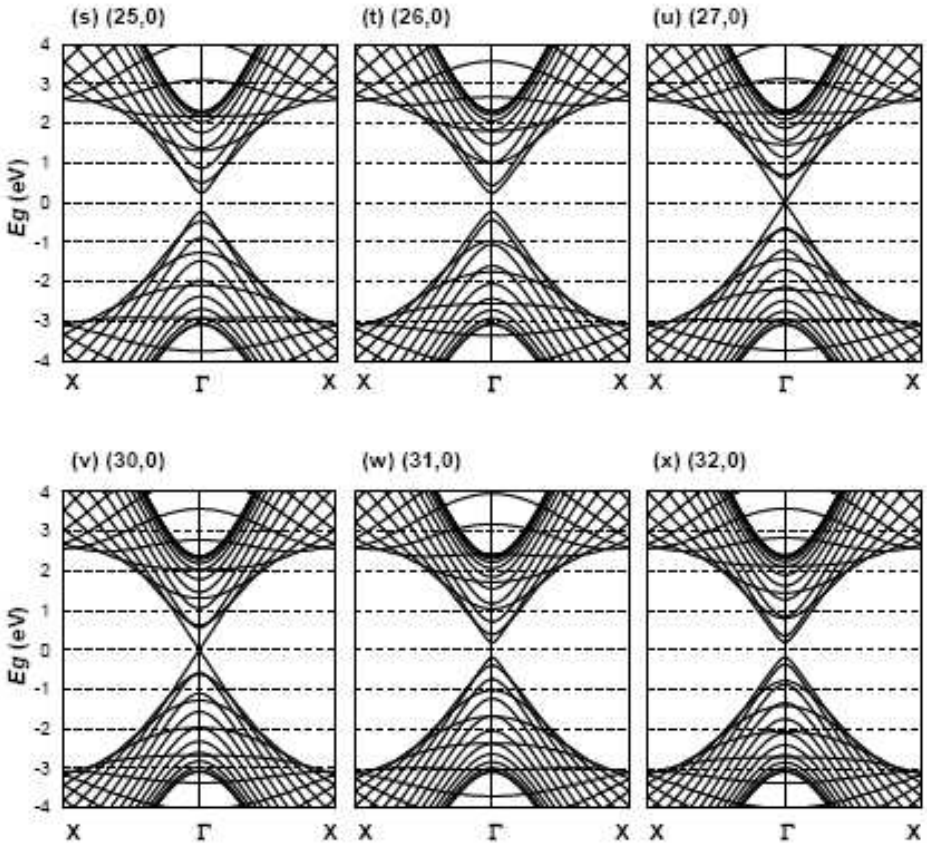

Figure S3-4. Band structures of zigazag SWNTs calculated using the B3LYP functional. (s) (25,0), (t) (26,0), (u) (27,0), (v) (30,0), (w) (31,0), and (x) (32,0).

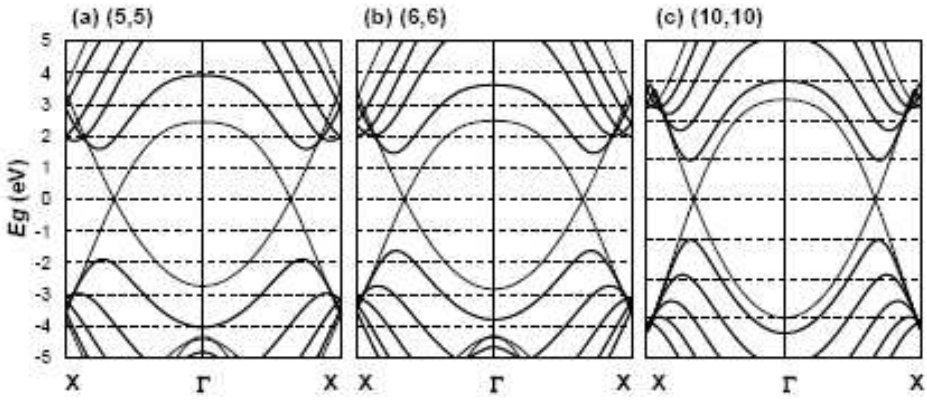

Figure S4. Band structures of armchair SWNTs calculated using the B3LYP functional. (a) (5,5), (b) (6,6), and (c) (10,10).

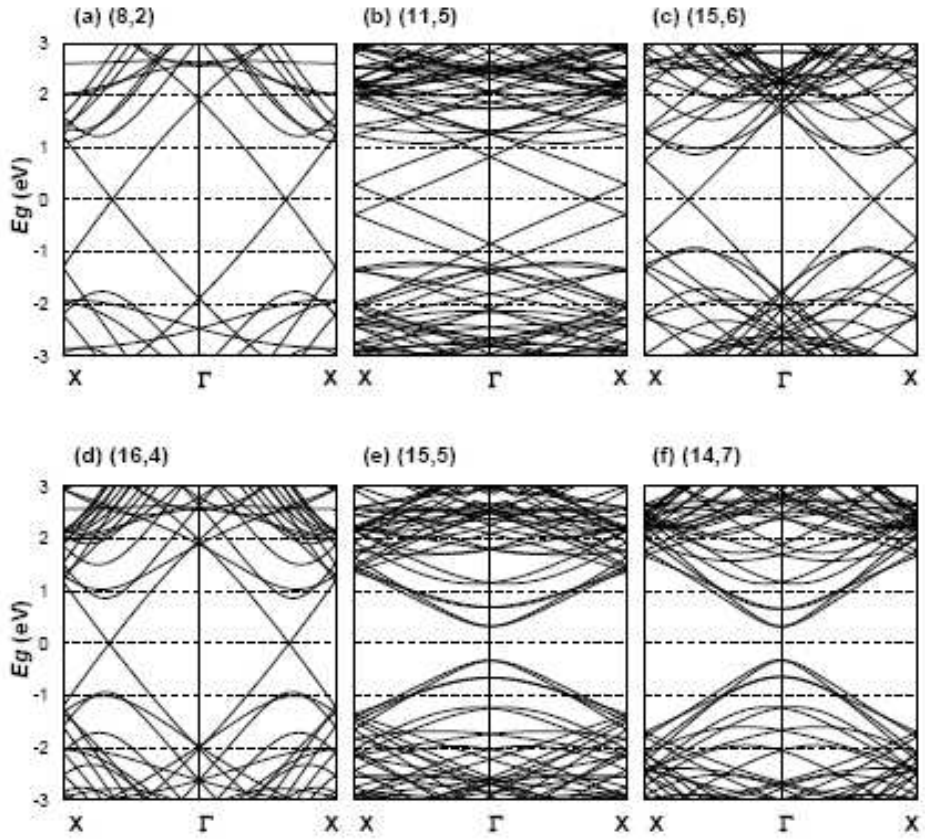

Figure S5. Band structures of chiral SWNTs of (a) (8,2), (b) (11,5), (c) (15,6), (d) (16,4), (e) (15,5), and (f) (14,7).